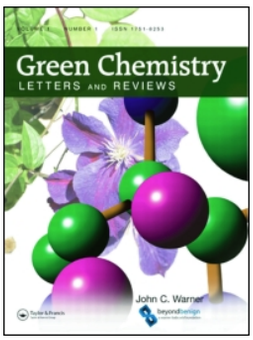

Green Chemistry Letters and Reviews

ISSN: 1751-8253 (Print) 1751-7192 (Online) Journal homepage: https://www.tandfonline.com/loi/tgcl20

Green synthesis of silver nanoparticles by *Ferulago macrocarpa* flowers extract and their antibacterial, antifungal and toxic effects

Farideh Azarbani & Sima Shiravand

To cite this article: Farideh Azarbani & Sima Shiravand (2020) Green synthesis of silver nanoparticles by *Ferulago macrocarpa* flowers extract and their antibacterial, antifungal and toxic effects, Green Chemistry Letters and Reviews, 13:1, 41-49, DOI: 10.1080/17518253.2020.1726504

To link to this article: https://doi.org/10.1080/17518253.2020.1726504

Published online: 18 Feb 2020.

GREEN CHEMISTRY LETTERS AND REVIEWS
2020, VOL. 13, NO. 1, 41–49
https://doi.org/10.1080/17518253.2020.1726504

Taylor & Francis
Taylor & Francis Group

LETTER

Green synthesis of silver nanoparticles by *Ferulago macrocarpa* flowers extract and their antibacterial, antifungal and toxic effects

Farideh Azarbani and Sima Shiravand

Department of Biology, Lorestan University, Khorramabad, Iran

ABSTRACT

Silver nanoparticles (SNPs) were phyto-synthesized from silver nitrate solution using the *Ferulago macrocarpa* flower extract. The UV–Visible, FT-IR, SEM, EDX, XRF and XRD analysis were used to characterize the SNPs. The optimum conditions of SNP synthesis were 1mM silver nitrate volume ratio 1.3, pH 11, temperature 80°C and incubation time 2.5 h. The dark brown color formation and UV-Visible spectrum with a characteristic peak at 429 nm confirmed the SNP synthesis. The FT-IR spectroscopy showed the capping of the SNPs by compounds contained in the extract. The average size of the spherical -shaped SNPs was 17 nm ranged between 14 and 25 nm. EDX and XRF spectra revealed a strong signal in the silver region. The SNPs exhibited activity towards *Staphylococcus aureus*, *Klebsiella pneumonia, Bacillus cereus*, *Escherichia coli,* and *Candida albicans*. However, they did not show toxicity on normal peripheral blood mononuclear cells at concentrations up to 250 µg/mL.

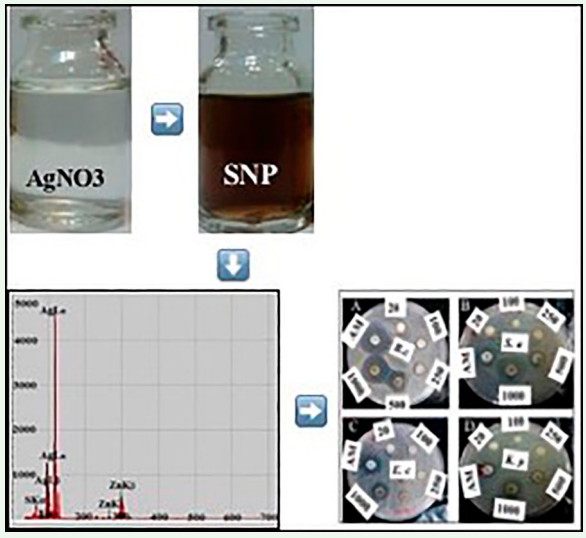

ARTICLE HISTORY
Received 6 April 2018
Accepted 30 January 2020

KEYWORDS
Ferulago macrocarpa; silver nanoparticle; antibacterial; antifungal; toxicity

1. Introduction

Nanoparticles (NPs) are small substances in the range of 1–100 nanometers in at least one dimension. They have a large surface to size ratio as opposed to bulk materials. This leads to their unique physical and chemical properties. For instance, the increased surface area of the nanoparticles enhances their chance to interact with surrounding molecules (*1*). Metallic NPs have a wide range of applications in areas such as catalysis, plasmonics, electronics, biotechnology, and medicine (*2–9*). Among noble metal NPs, silver nanoparticles (SNPs) play a significant role in the medicinal field. Their antibacterial, antifungal, antioxidant, anti-inflammatory, anti-angiogenesis, and anti-cancer activities have been reported (*10–14*). Due to their high antimicrobial properties, they have been incorporated into a wide array of consumer products including wound dressings, clothing, cosmetics, paints, apparel, footwear, and appliances (*15*,*16*). There are a variety of chemical and physical approaches to the production of NPs. However, overall

CONTACT Farideh Azarbani frazarban@gmail.com, Azarbani.f@lu.ac.ir

these methods are expensive, time-consuming, energy-demanding and not eco-friendly. Thus, there is a growing interest to develop fast, economical and eco-friendly procedures to nanoparticle synthesis. In recent years, the biosynthesis of NPs using natural resources including microorganisms, plant extracts, polymers, sugars and enzymes as reductants and capping agents has been achieved (*17–20*). Biosynthesis of NPs has many advantages over other methods. It is simple, cost-effective, eco-friendly, and there is no need to use high energy, pressure, temperature and toxic chemicals (*21*). From biological alternatives, plants seem to be the best candidates. They are easily available, safe in most cases, have an extensive diversity of secondary metabolites, are faster than other organisms in the synthesis, and the produced NPs are often stable (*22, 23*). Various plants like *Myrmecodia pendans*, *Tectona grandis*, *Syzygium cumini*, *Rhynchotechum ellipticum*, *Alternaria alternate, Ziziphora tenuior, Beetroot,* and *Erythrina indica* have been used successfully in the biosynthesis of nanosilver (*24–31*). Different parts of plants such as leaf, flower, stem, fruit, seed, shoot, bark, peel, root and callus have been studied in this direction (*32–37*). *Ferulago macrocarpa* (Fenzl) Boiss, known as Chavil-e-Roshan ball in Farsi, is a wild medicinal plant from the Apiaceae family which grows in the west of Iran and is used as traditional medicine, food protectant, and flavoring agent (*38–40*). The present study aims at the biosynthesis of SNPs using *F. macrocarpa* flower aqueous extract and evaluation of their antibacterial, antifungal and toxicity effects.

2. Experimental procedure

2.1. F. macrocarpa *extract preparation*

The plant was collected from its local region in Lorestan province, Iran. It was washed with tap water, followed by distilled water and then shade-dried at room temperature.

The dried *F. macrocarpa* flowers were powered with the help of a grinder. Ten grams of powder was mixed with 100 ml of deionized water in a 250 ml Erlenmeyer flask and heated in a water bath at 80°C for 40 min. After cooling down, the mixture for 20 min at 12,000 rpm was centrifuged. The supernatant was filtered and kept at 4°C for further analysis.

2.2. Antioxidant assay

Antioxidant capacity of the *F. macrocarpa* flower extract was evaluated regarding DPPH (1, 1- diphenyl-2-picrylhydrazyl) radical scavenging activity (RSA) and calculated as follows (*41*):

$$\mathrm{RSA}(\%) = \frac{(A_c - A_s)}{A_c} \times 100.$$

A_C is the absorbance of the DPPH solution as control and A_S is the absorbance of DPPH solution in the presence of the extract. The extract concentration required to neutralize 50% of DPPH radicals was measured as IC50.

2.3. Preparation of silver nanoparticles (SNPs)

The *F. macrocarpa* flower extract was mixed with 1mM silver nitrate solution in different volume ratios (1:1, 1:2, 1:4, 3:4 and 3:2), reaction pH (4.5,7, 9 and 11) and temperature (30°C, 60°C and 80°C). The mixture was incubated in darkness to complete the reaction. The formation of silver nanoparticles in the reaction mixture was monitored by visual observation and Ultraviolet–Visible (UV-Vis) spectroscopy at different reaction time intervals. The precipitated particles were separated by centrifuging at 10,000 rpm for 20 min, washed with deionized water by repeated centrifugation and dried in the oven at 60°C.

2.4. Characterization of synthesized SNPs

The formation of SNPs was periodically monitored by measuring the UV-Visible spectrum of the NP suspension diluted with an equal volume of deionized water using JENWAY 6405 spectrometer at 350–700 nm. Fourier transform infrared (FT-IR) analysis was performed to identify biomolecules that could play a role in the reduction of silver ions or capping of the resulting SNPs. FT-IR spectra were recorded on Shimadzu 8400S spectrophotometer using the potassium bromide (KBr) technique at 400–4000 cm^{-1} with 4 cm^{-1} resolution. The surface morphology and size of the NPs were determined with Tescan Mira 3 LMU Scanning electron microscope (SEM) equipped with Energy-dispersive X-ray (EDX) spectroscopy at 15 kV with 1 nm resolution. The crystalline structure of the NPs was determined by a Philips X'Pert Pro MPD X-ray diffractometer in a 2-theta range of 20°–80° with Cu Kα radiation. A GNR TX2000 X-ray fluorescence spectrometer (XRF) was used to define the composition of materials.

2.5. Antimicrobial activity of SNPs

The antibacterial capacity of produced SNPs was assayed on *Escherichia coli* (ATCC 8739), *Bacillus cereus* (ATCC 11778), *Klebsiella pneumonia* (ATCC 10031) and

Staphylococcus aureus (ATCC 6538) using disc diffusion method (42). The suspension of overnight bacterial culture was adjusted to 0.5 McFarland solution and swabbed on the Muller Hinton Agar (MHA) petri dishes. The impregnated discs with 35 µL of different concentrations of the SNPs colloidal suspension (20–1000 µg/mL) were placed on the inoculated dishes surface. Following 24 h maintenance at 37°C, the diameter of inhibition holes was measured (mm). The minimum inhibitory concentrations (MICs) were evaluated by the broth microdilution method (43). The minimum bactericidal concentrations (MBCs) were then determined.

Antifungal property of the SNPs was also tested against *Candida albicans* (PTCC 10261) by agar well diffusion method (44). The *C. albicans* suspension was swabbed on the sabouraud dextrose agar dishes. The 6 mm diameter wells were punched on the surface of the sabouraud dextrose agar dishes. Each well was filled with 60 µL of the SNPs colloidal suspension at different concentrations (50–1000 µg/mL). The dishes were then kept at 35°C for 48 h. By measuring the diameter of inhibition holes, the antifungal function of the particles was determined. The lowest SNP concentration that resulted in visual inhibition of fungal growth was considered as minimum inhibitory concentration (MIC).

2.6. Toxicity test

Peripheral blood mononuclear cells (PBMCs) isolated from healthy blood donors were cultured in 96-well flat-bottom plate at a concentration of 2×10^4 cells per well. After 4-h spreading, the cells were exposed to the SNPs suspension and kept in a humidified atmosphere with 5% CO_2 at 37°C for 24 h. At the end of the treatment period, the cell viability was detected by methyl thiazolyl diphenyl tetrazolium bromide (MTT) assay (45). The percentage of viable cells was calculated using the following formula:

$$\text{Cell Viability}(\%) = \left(\frac{\text{Absorbance of Treatment}}{\text{Absorbance of Control}}\right) \times 100.$$

A concentration of the SNPs that inhibits the growth of cells over 50% was considered to be toxic (46).

2.7. Statistical analysis

The experiments were performed in triplicate, and the results expressed as means ± SD. Statistical analyses were performed using one-way ANOVA by SPPS version 15.0 and Excel 2016. The *p*-values of less than 0.05 were regarded as significant.

3. Results and discussion

3.1. Synthesis of SNPs

The *F. macrocarpa* flower extract exhibited significant antioxidant activity with a DPPH IC50 value of 378.4 ± 0.1 µg/mL. Thus, its aqueous extract was used as a reducing agent in nanosilver synthesis. To derive the optimum conditions for SNP synthesis, the *F. macrocarpa* flower extract and 1mM silver nitrate solution were mixed at different ratios. These mixtures having pH value around 4 were incubated at room temperature. With the passage of time, the color of the solution changed slowly from colorless to yellowish-brown and finally dark brown, which may be due to the excitation of surface plasmon vibrations in SNPs. To examine the formation of nanoparticles, a small amount of the mixtures was diluted with deionized water (1:1) and monitored by measuring UV-Visible spectra at different time intervals. After overnight incubation, the absorbance peaks around 390–410 nm were formed. As shown in Figure 1(a), with increasing the silver nitrate volume ratio, the absorption peak shifted towards lower wavelength, indicating a decrease in the particle size (47). At the volume ratio of 4:3, a narrow band was observed. This ratio was further used for optimization purposes.

To investigate the influence of temperature on nanoparticle synthesis, the reaction was carried out at various temperatures in the range of 30°C–80°C. As the reaction temperature increases, a faster change in the samples color occurred, the absorption intensity increased, and the absorption band shifted towards lower wavelength (Figure 1(b)). Increasing the reaction temperature increases the kinetic energy of the molecules, which result in faster consumption of silver ions, and thus leaving less possibility for particle size growth (48).

The medium pH was another factor that affected the rate of reaction. To study the effect of pH on the synthesis of SNPs, the extract and 1mM silver nitrate solution were adjusted to different pH and mixed 4:3 (*v/v*) at 80°C. By increasing the reaction pH, the absorbance band exhibited a red shift from 410 to 429 nm (Figure 1(c)). An enhancement in absorption intensity was also observed. Changing the reaction pH alter the electrical charges of biomolecules which might affect their reducing and capping abilities and subsequently the NPs growth (49).

The results indicated the presence of both alkaline pH and high temperature are more favorable for the SNPs synthesis using the *F. macrocarpa* flower aqueous extract. The maximum surface plasmon resonance band intensity was detected at pH 11 after 2.5 h

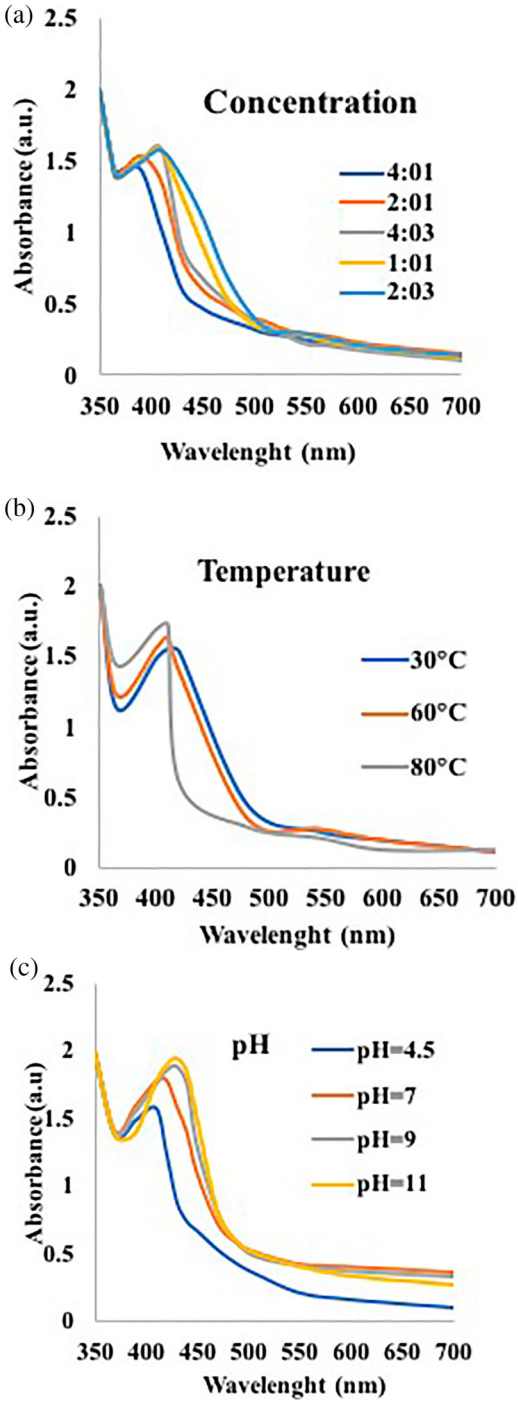

Figure 1. (a) Absorption spectra of the SNPs colloidal solution obtained at the various volume ratio of 1 mM silver nitrate. (b) Absorption spectra of the SNPs colloidal solution obtained at different reaction temperatures. (c) Absorption spectra of the SNPs colloidal solution obtained at different reaction pH.

incubation at 80°C. The formed NPs showed a sharp absorption peak at around 429 nm specific for SNPs. The sharp peak demonstrates spherical shape SNP synthesis [20]. The color and absorbance of the solution did not change after this time. This absorbance peak even after 21 days was observed, indicating the stability

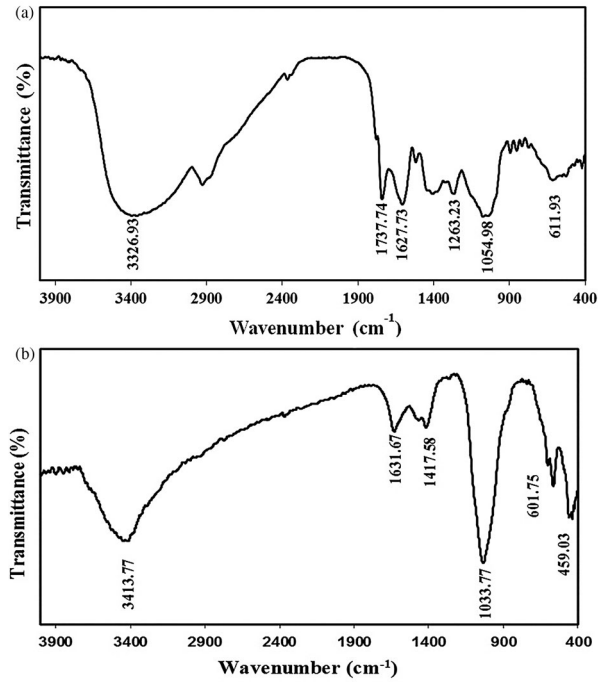

Figure 2. (a) FT-IR pattern of the *F. macrocarpa* flower extract. (b) FT-IR pattern of the phyto-synthesized SNPs.

of NPs. It is concluded that *F. macrocarpa* flowers extract acts as both reducing and stabilizing agents.

FT-IR spectroscopy was used to identify the compounds in the extract which may act as a reducing agent for Ag^+ ions or as the SNP capping agent.

In Figure 2(a), *F. macrocarpa* extract displays the main absorbance bands at about 3326, 1627, 1407 and 1054 cm^{-1}. The broadband at 3326 cm^{-1} is due to O-H stretching in alcohols and phenols or N-H stretching of amines. The bands at 1627 and 1407 cm^{-1} arises from the C=O stretching in carbonyl group and -C–O stretching of esters, respectively. The existence of a band at 1054 cm^{-1} is probably related to -C–O-C- stretching mode (*50–52*). As shown in Figure 2(b), the FT-IR absorbance peaks of the SNPs have a high degree of similarity to those of the *F. macrocarpa* flower extract, for instance, the peaks at about 3413, 1631, 1417 and 1033 cm^{-1}. The shift in the bands revealed that silver nitrate was reduced by biomolecules present in the extract. The presence of the hydroxyl (–OH), amine (N-H) and carbonyl (–C=O) groups in the extract proposing that the compounds like phenolics, terpenoids and proteins are involved in the synthesis, capping and stabilizing of the SNPs. The existence of terpenoids like terpinolene, limonene, pinene and selinene in the *F. macrocarpa* flowers essential oil was confirmed by GC/MS analysis (data not shown). The phenolics and proteins in the extract may act as a reducing agent to produce nanoparticles from silver nitrate, and coating agent for stabilization of the SNPs, respectively.

The proposed mechanism for the synthesis of SNPs using *F. macrocarpa* flower extract may be explained as follow: the silver ion in the silver nitrate solution is possibly attacked by the oxygen atom of the phenolics or terpenoids hydroxyl group leading to the formation of an atomic form of silver. Also, the proteins containing the carboxyl group have a potent chelating ability with metal, signifying the formation of a covering layer on SNPs and thus acting as a capping and stabilizing agent to protect the agglomeration of NPs. Therefore, the possible mechanism suggests that the phenolics or terpenoids present in the extract are involved in the reduction of silver ions, and the proteins are responsible for the capping and stabilization of SNPs.

The morphological shape and size of synthesized NPs were investigated by the SEM method. The SEM images show the NPs are mostly spherical which agrees with UV-Vis results. The particles diameter ranged between 14 and 25 nm (Figure 3).

Similar to our study, the SNPs synthesized using aqueous flower extract of *Cassia angustifolia* exhibited spherical shape with different sizes range from 10 to 80 nm (*53*). Nadagouda et al. (*54*) reported that the size of nanosilver synthesized using the antioxidant constituents depends on the nature of extract and method of preparation.

The EDX spectrum of prepared NPs shows an intense optical absorption peak at about 3 keV which is typical for metallic SNPs (*55*). Nearly 89% of nanosilver was detected from EDX. The major contaminants are nitrogen (9.1%) and sulfur (1.2%) that may originate from the proteins that are bound to the surface of the SNPs (Figure 4).

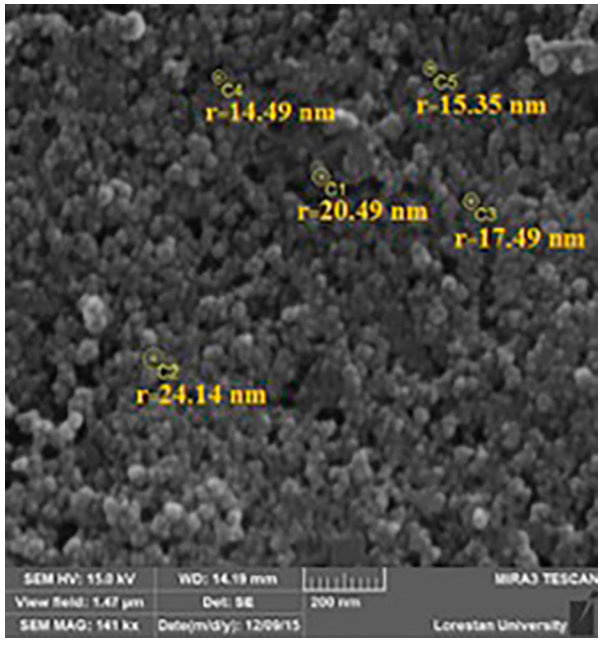

Figure 3. SEM image of the SNPs.

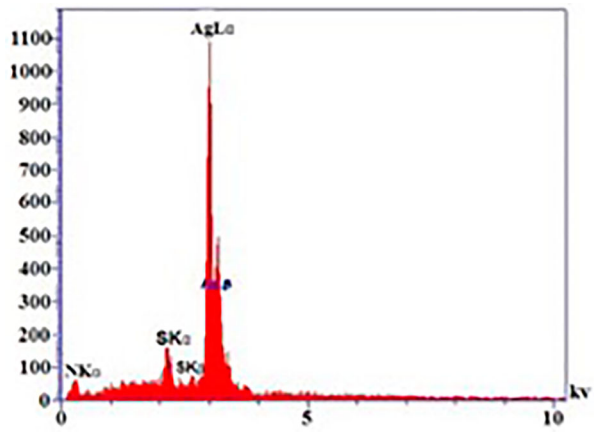

Figure 4. EDX image of the SNPs.

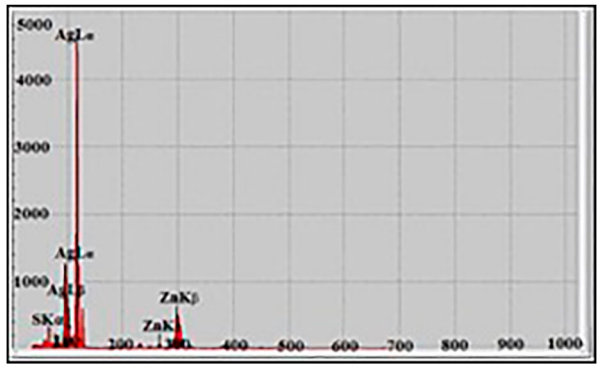

Figure 5. XRF image of the SNPs.

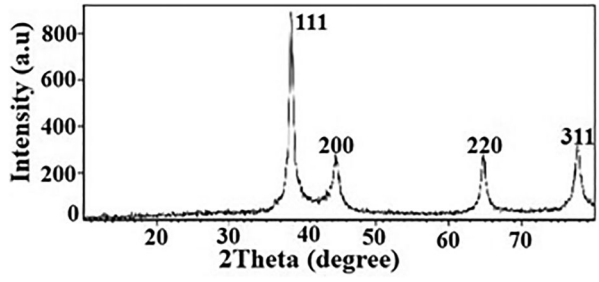

Figure 6. XRD pattern of the SNPs.

The X-ray fluorescence analysis indicated the existence of silver as a major constituent element. The elemental impurities in the sample were sulfur (14.79%) and zinc (0.06%) (Figure 5).

XRD analysis was performed to confirm the crystalline structure and the estimated size of synthesized particles by the *F. macrocarpa* extract. As shown in Figure 6, the XRD spectrum of SNPs exhibits four sharp and distinct

diffraction peaks at 2θ values of 38.45°, 44.54°, 64.64° and 77.65°, which correspond to 111, 200, 220 and 311 crystallographic planes of silver (*56*). The XRD spectrum confirms the crystal structure of SNPs (*57*). The average crystalline size of SNPs was calculated from the XRD data using the Debye-Scherrer equation ($d = k.\ \lambda\ /\ \beta.\ \text{Cos}\ \theta$). Where d is the particle size of the crystal, k is Sherrer constant (0.9), λ is the wavelength of X-ray source used in XRD (0.15406 nm), β is the breadth of the observed diffraction peak at its half maximum and θ is the Bragg angle. From Scherrer's equation, the average crystallite size of synthesized SNPs was 17 nm, which is in agreement with the particle size measured from SEM. The impurity peaks were not observed in XRD patterns.

3.3. Antimicrobial activity

The SNPs exhibited activity against all tested bacteria. The maximum non-growth halo diameter was 17 mm in *B. cereus* bacteria followed by *S. aureus, E. coli,* and *K. Pneumonia.* Antibacterial activities were dose-dependent and increased with the SNP concentration (Figure 7).

Table 1 shows that the results obtained from the broth microdilution method corresponded to the disk diffusion test results, where the antibacterial activity of the SNPs was higher against the mentioned Gram-positive bacteria than the negatives. The synthesized SNPs had both MIC and MBC values of 62.5 µg/mL toward *B. cereus* bacterium.

Table 1. Antibacterial activity of the SNPs colloidal suspension.

Bacteria	*Zone of inhibition* (mm) Concentration (µg/mL)				MIC (µg/mL)	MBC (µg/mL)
	100	250	500	1000		
S. aureus	8 ± 0.1	9 ± 0.3	12 ± 0.5	15 ± 0.4	62.5	125
B. cereus	10 ± 0.5	11 ± 0.4	15 ± 0.4	17 ± 0.7	62.5	62.5
E. coli	8 ± 0.1	9 ± 0.4	11 ± 0.6	14 ± 0.3	250	250
K. Pneumonia	–	8 ± 0.4	10 ± 0.5	12 ± 0.2	250	500

In the present study, the phyto-synthesized SNPs were found to be more effective against the tested Gram-positive bacteria than the negatives. The similar results were found for the biogenic SNPs using bacteria (*58*) and latex of *Syandenium grantii* Hook f (*59*). Madakka et al. found that mycogenic silver nanoparticles have more potent antibacterial activity against *S. aureus* than *E. Coli* (*60*), whereas some researchers have reported the reverse results (*61–63*).

Several studies have demonstrated the antibacterial potential of silver nanoparticles is affected by their

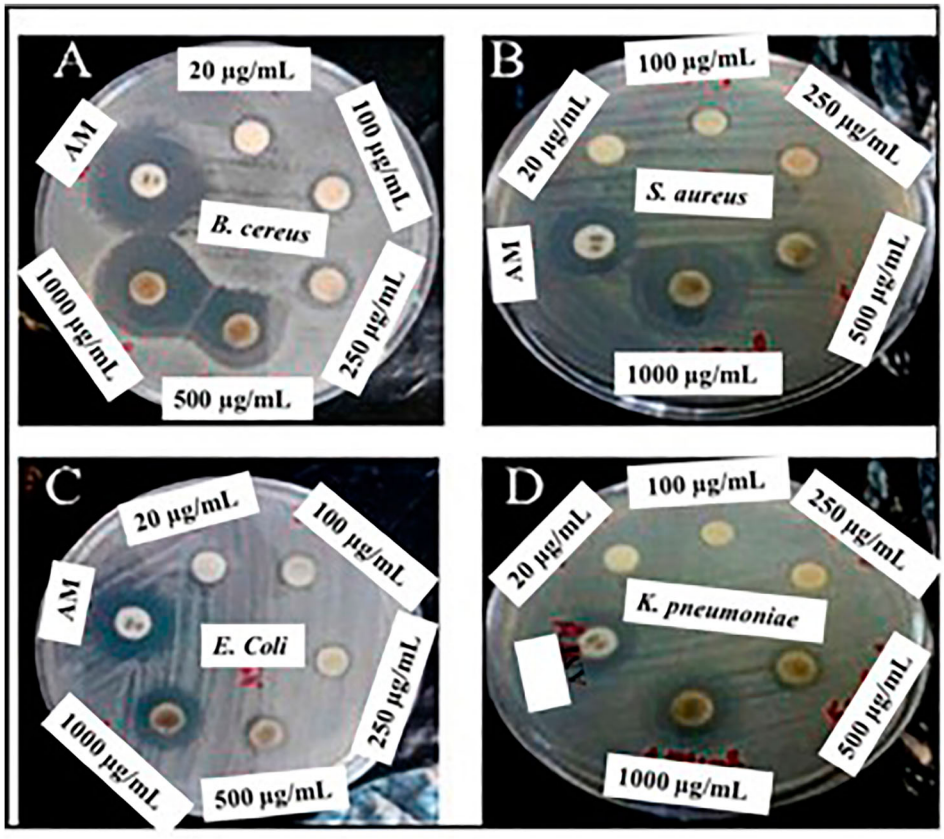

Figure 7. Antibacterial activity of the SNPs against: (A) *B. cereus*, (B) *S. aureus*, (C) *E. coli*, (D) *K. Pneumonia.* Amikacin (AM) was used as a standard.

shape, size, surface charge, concentration, and colloidal state (*64, 65*). Furthermore, parameters such as the nature of plant extract, pH, and reaction time strongly affect the size, shape, and morphology of the AgNPs (*66*). However, the specific response of each bacterium depended on its metabolic characteristics.

Although an exact mechanism behind the biocidal activity of SNPs is not yet fully known, several probable mechanisms have been reported. It was suggested that the toxicity of SNPs might be attributed to free radicals derived from the surface of the nanoparticles, causing a significant increase in membrane permeability and leading to cell death (*67*). It is also suggested that in the bacterial cells silver ions released from the SNPs may interact with negatively charged phosphorus and sulfur in macromolecules like DNA and proteins to distort them. This leads to disturbances in metabolic processes and eventual cell death (*68*).

The phyto-synthesized SNPs also showed significant antifungal activity against *C. albicans* with a MFC value of 500 µg/mL (Figure 8).

3.4. Toxicity assay

The effect of the bio-synthesized SNPs was studied on the human PBMCs by the MTT method at concentrations close to their MIC values (50 and 250 µg/mL). After 24 h of treatment, the viability of cells treated with SNPs decreased slightly to about 90% compared to that shown by control cells. The SNPs exhibited about 10% and 13% cell lysis at 50 and 250 µg/mL, respectively. Therefore, the SNPs synthesized by *F. macrocarpa* flower extract at the minimum inhibitory concentration did not have a significant toxic effect on peripheral blood cells. It was reported by Borase et al. (*69*) that SNPs synthesized by *J. gossypifolia* extract showed amoebicidal activity, but they were nontoxic at the minimum inhibitory concentration with PBM cells. The SNPs at 50 µg/mL exhibited the maximum PBMCs inhibition (22%). Barua et al. (*70*) have also reported that SNPs synthesized by *Thuja occidentalis* leaf extract exhibited anticancer activity against human breast and cervical cancer as well as mouth epidermoid carcinoma cell lines at a concentration range of 6.25–50 µg/mL, but they were compatible with human peripheral blood mononuclear cells and rat hepatocytes. In another study, SNPs synthesized by glucose in the presence of PVP showed toxicity at 25 µg/mL and higher on monocytes. However, no toxic effects on the T-cells were observed in the presence of these concentrations of SNPs (*71*). Some researchers have reported the toxicity of the plant-mediated SNPs on human healthy cells (*72, 73*). In general, the toxicity of SNPs depends not only on the cell type but also on factors like particle shape, size, surface charge and the capping agent (*74*).

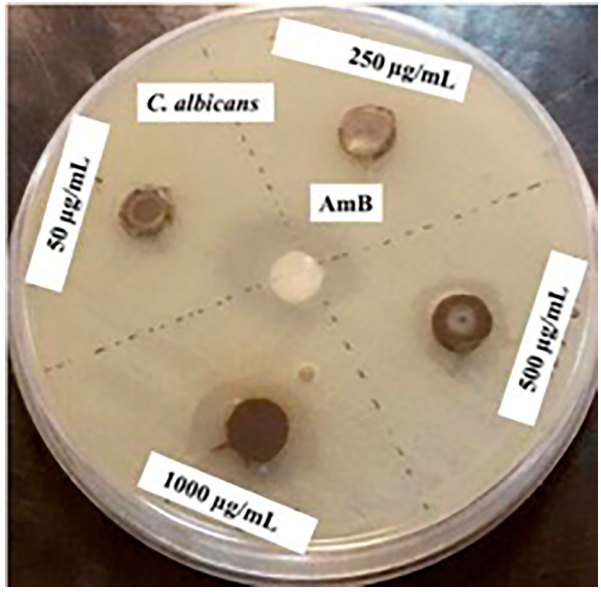

Figure 8. Antifungal activity of the SNPs against *C. albicans*. Amphotericin B (AmB) was used as a standard.

4. Conclusions

In the current investigation, we reported a rapid, low cost and environment-friendly procedure for the synthesis of SNPs from silver nitrate salt using *F. macrocarpa* flower aqueous extract. In this method, stable SNPs with a high yield of 89% in the size range of 14–25 nm were produced.

The size of these nanoparticles could be controlled by varying the extract concentration, reaction temperature, and pH. Phenolic compounds in the extract are possibly involved in the silver ions reduction, and the proteins act as capping and stabilizing agents. The phyto-synthesized SNPs exhibited toxicity against both tested Gram-positive and negative bacteria that are usually involved in hospital-acquired infections. The SNPs also displayed antifungal activity against *C. albicans*. However, they did not show significant toxicity on human normal peripheral blood mononuclear cells at concentrations equal to MIC values. The coating of the extract biomolecules on the surface of the SNPs probably reduces their toxicity. Thus, the synthesized SNPs may be used in the treatment and prevention of bacterial infections.

Acknowledgements

Thanks to the Research Deputy of Lorestan University, Iran, for funding this project (grant # 954044895). We also thank Mr. G. Veiskarami for his help in identifying the plant.

Disclosure statement

No potential conflict of interest was reported by the author(s).

Notes on contributors

Farideh Azarbani received the M.Sc degree in biochemistry from Faculty of Medical Sciences, Tarbiat Modares University, Iran, in 2000. She received the Ph.D degree in biochemistry from Tehran University, Iran, in 2007. Since then, she has been with Department of Chemistry (2007–2010) and Department of Biology (from 2010 to now), Lorestan University, Iran, where she is currently an associate professor. Her main areas of research interest are medicinal chemistry, Antibiotics, green chemistry and medicinal plants.

Sima Shiravand received the Bachelor degree in biology from Payame Noor University, Khorramabad, Iran, in 2011. She received the M.Sc degree in biochemistry from Lorestan University, Iran, in 2015. She has worked as a research assistant in the Biology Laboratory of Lorestan University for several years. Her main areas of research interest are Antibiotics, green synthesis and medicinal plants.

Funding

This work was supported by Research Deputy of Lorestan University, Iran [grant number 954044895].

References

[1] Sampath, M.; Vijayan, R.; Tamilarasu, E.; Tamilselvan, A.; Sengottuvelan, B. *J. Nanotechnol.* **2014,** *33*, 1–7.
[2] Fardood, S.T.; Ramazani, A.; Moradi, S. *J. Sol-Gel Sci.* **2017,** *82*, 432–439.
[3] Malekzadeh, A.M.; Shokrollahi, S.; Ramazani, A.; Rezaei, S.J.; Asiabi, P.A.; Joo, S.W. *Cent. Eur. J. Energ. Mater.* **2017,** *14*, 336–351.
[4] Fodjo, E.K.; Gabriel, K.M.; Serge, B.Y.; Li, D.; Kong, C.; Trokourey, A. *Chem. Cent. J.* **2017,** *11*, 58–67.
[5] Huergo, M.A.; Giovanetti, L.; Moreno, M.S.; Maier, C.M.; Requejo, F.G.; Salvarezza, R.C.; Vericat, C. *Langmuir* **2017,** *33*, 6785–6793.
[6] Violi, I.L.; Gargiulo, J.; Von Bilderling, C.; Cortés, E.; Stefani, F.D. *Nano Lett.* **2016,** *16*, 6529–6533.
[7] Gontero, D.; Veglia, A.V.; Bracamonte, A.G.; Boudreau, D. *RSC Adv.* **2017**, *7*, 10252–10258.
[8] Khatoon, N.; Mazumder, J.A.; Sardar, M. *J. Nanosci. Curr. Res.* **2017,** *2*, 1–2.
[9] Elemike, E.E.; Onwudiwe, D.C.; Ekennia, A.C.; Sonde, C.U.; Ehiri, R.C. *Molecules* **2017,** *22*, 674–689.
[10] Bahrami-Teimoori, B.; Nikparast, Y.; Hojatianfar, M.; Akhlaghi, M.; Ghorbani, R.; Pourianfar, H.R. *J. Exp. Nanosci.* **2017,** *12*, 129–139.
[11] Elemike, E.E.; Fayemi, O.E.; Ekennia, A.C.; Onwudiwe, D.C.; Ebenso, E.E. *Molecules* **2017,** *22*, 701–720.
[12] Gomaa, E.Z. *J. Genet. Eng. Biotechnol.* **2017,** *15*, 49–57.
[13] Baharara, J.; Namvar, F.; Mousavi, M.; Ramezani, T.; Mohamad, R. *Molecules* **2014,** *19*, 13498–13508.
[14] Mani, A.K.; Seethalakshmi, S.; Gopal, V. *J. Nanomed. Nanotechnol.* **2015,** *6*, 1–5.
[15] Mavani, K.; Shah, M. *IJLRET* **2013**, *2*, 1–5.
[16] Zhang, X.F.; Liu, Z.G.; Shen, W.; Gurunathan, S. *Int. J. Mol. Sci.* **2016,** *17*, 1534–1568.
[17] Ahmed, S.; Ahmad, M.; Ikram, S. *JOAC* **2014**, *3*, 493–503.
[18] Thapa, R.; Bhagat, C.; Shrestha, P.; Awal, S.; Dudhagara, P. *Ann. Clin. Microbiol. Antimicrob.* **2017,** *16*, 39–49.
[19] Sadowski, Z.; Maliszewska, I.H.; Grochowalska, B.; Polowczyk, I.; Kozlecki, T. *MATER. SCI.-POLAND* **2008**, *26*, 419–424.
[20] Eising, R.; Elias, W.C.; Albuquerque, B.L.; Fort, S.; Domingos, J.B. *Langmuir* **2014**, *30*, 6011–6120.
[21] Iravani, S.; Korbekandi, H.; Mirmohammadi, S.V.; Zolfaghari, B. *Res. Pharm. Sci.* **2014,** *9*, 385–406.
[22] Janaki, A.C.; Sailatha, E.; Gunasekaran, S. *Spectrochim. Acta A.* **2015,** *144*, 17–22.
[23] Prabhu, S.; Poulose, E.K. *Int. Nano. Lett.* **2012,** *2*, 32–41.
[24] Zuas, O.; Hamim, N.; Sampora, Y. *Mater. Lett.* **2014,** *123*, 156–159.
[25] Nalvothula, R.; Nagati, V.B.; Koyyati, R.; Merugu, R.; Padigya, P.R. *Int. J. ChemTech. Res.* **2014,** *6*, 293–298.
[26] Mittal, A.K.; Bhaumik, J.; Kumar, S.; Banerjee, U.C. *J. Colloid Interface Sci.* **2014,** *415*, 39–47.
[27] Hazarika, D.; Phukan, A.L.; Saikia, E.; Chetia, B. *Int. J. Pharm. Sci.* **2014,** *6*, 672–674.
[28] Baharvandi, A.; Soleimani, M.J.; Zamani, P. *Arch. Phytopathol. Plant Protect* **2015,** *48*, 313–318.
[29] Sadeghi, B.; Gholamhoseinpoor, F. *Spectrochim. Acta A.* **2015,** *134*, 310–315.
[30] Bindhu, M.R.; Umadevi, M. *Spectrochim. Acta A.* **2015,** *135*, 373–378.
[31] Sre, P.R.; Reka, M.; Poovazhagi, R.; Kumar, M.A.; Murugesan, K. *Spectrochim. Acta A.* **2015,** *135*, 1137–1144.
[32] MubarakAli, D.; Thajuddin, N.; Jeganathan, K.; Gunasekaran, M. *Colloids Surf. B* **2011,** *85*, 360–365.
[33] Prathna, T.C.; Chandrasekaran, N.; Raichur, A.M.; Mukherjee, A. *Colloids Surf. B* **2011,** *82*, 152–159.
[34] Sathish kumar, M.; Sneha, K.; Won, S.W.; Cho, C.W.; Kim, S.; Yun, Y.S. *Colloids Surf. B* **2009,** *73*, 332–338.
[35] Bankar, A.; Joshi, B.; Kumar, A.R.; Zinjarde, S. *Colloids Surf. A* **2010,** *368*, 58–63.
[36] Ahmad, N.; Sharma, S.; Alam, M.K.; Singh, V.N.; Shamsi, S.F.; Mehta, B.R.; Fatma, A. *Colloids Surf. B* **2010,** *81*, 81–86.
[37] Nabikhan, A.; Kandasamy, K.; Raj, A.; Alikunhi, N.M. *Colloids Surf. B* **2010,** *79*, 488–493.
[38] Rafieian-kopaei, M.; Shahinfard, N.; Rouhi-Boroujeni, H.; Gharipour, M.; Darvishzadeh-Boroujeni, P. *Evid Based Complement Alternat. Med.* **2014,** *2014*, 1–4.
[39] Ghasemi, P.A.; Momeni, M.; Bahmani, M. *Afr. J. Tradit Complement Altern. Med.* **2013,** *10*, 368–385.
[40] Sajjadi, S.; Shokoohinia, Y.; Jamali, M. *Res. Pharm. Sci.* **2012,** *7*, 197–200.
[41] Zakaria, Z.; Aziz, R.; Lachimanan, Y.L.; Sreenivasan, S.; Rathinam, X. *Int. J. Nat. Eng. Sci.* **2008,** *2*, 93–95.
[42] Li, Z.; Lee, D.; Sheng, X.; Cohen, R.E.; Rubner, M.F. *Langmuir* **2006,** *22*, 9820–9823.
[43] Engelkirk, P.G.; Duben-Engelkirk, J.L. *Laboratory Diagnosis of Infectious Diseases: Essentials of Diagnostic Microbiology*; LWW: Baltimore, 2008; pp 168–169.
[44] Yigit, N.; Aktas, E.; Ayyildiz, A. *J. Mycol. Med.* **2008,** *18*, 141–146.
[45] Mosmann, T. *J. Immunol. Methods* **1983,** *65*, 55–63.
[46] Cole, S.P. *Cancer Chemother. Pharmacol.* **1986,** *17*, 259–263.
[47] Saware, K.; Venkataraman, A. *J. Clust. Sci.* **2014,** *25*, 1157–1171.

[48] Verma, A.; Mehata, M.S. *J. Rad. Res. Appl. Sci.* **2016,** *9*, 109–115.
[49] Khalil, M.M.H.; Ismail, E.H.; El-Baghdady, K.Z.; Mohamed, D. *Arab. J. Chem.* **2014,** *7*, 1131–1139.
[50] Rajathi, K.; Sridhar, S. *Int. J. Chem. Tech. Res.* **2013,** *5*, 1707–1713.
[51] Rastogi, L.; Arunachalam, J. *Mat. Chem. Phys.* **2011,** *129*, 558–563.
[52] Shankar, S.S.; Ahmad, A.; Sastry, M. *Biotechnol. Prog.* **2003,** *19*, 1627–1631.
[53] Devaraj Bharathi, D.; Bhuvaneshwari, V. *BioNanoSci.* **2019,** *9*, 155–163.
[54] Nadagouda, M.N.; Iyanna, N.; Lalley, J.; Han, C.; Dionysiou, D.D.; Varma, R.S. *ACS SUSTAIN CHEM ENG.* **2014,** *2*, 1717–1723.
[55] Kohler, J.M.; Csáki, A.; Reichert, J.; Möller, R.; Straube, W.; Fritzsche, W. *Sens. Actuators B Chem.* **2001,** *76*, 166–172.
[56] Bar, H.; Bhui, D.K.; Sahoo, G.P.; Sarkar, P.; De, S.P.; Misra, A. *J. Colloids Surf. A: Physicochem. Eng.* **2009,** *339*, 134–139.
[57] Raffi, M.; Hussain, F.; Bhatti, T.M.; Akhter, J.I.; Hameed, A.; Hasan, M.M. *J. Mater. Sci. Technol.* **2008,** *24*, 192–196.
[58] Joanna, C.; Marcin, L.; Ewa, K.; Grażyna, P. *Ecotoxicology* **2018**, *27*, 352–359.
[59] Durgawale, P.P.; Phatak, R.S.; Hendre, A.S. *Dig. J. Nanomater. Bios.* **2015,** *10*, 847–853.
[60] Madakka, M.; Jayaraju, N.; Rajesh, N. *MethodsX.* **2018,** *5*, 20–29.
[61] Zhang, M.; Zhang, K.; Gusseme, B.D.; Verstraete, W.; Field, R. *BIOFOULING* **2014,** *30*, 347–357.
[62] Dehnavi, A.S.; Raisi, A.; Aroujalian, A. *SYNTH REACT INORG M* **2013,** *43*, 543–551.
[63] Bharathi, D.; Josebin, M.D.; Vasantharaj, S.; Bhuvaneshwari, V. *JNSC* **2018,** *8*, 83–92.
[64] Dakal, T.C.; Kumal, N.; Majumdal, R.; Yadav, V. *Front. Microbiol.* **2016**, *7*, 1831.
[65] Hong, X.; Wen, J.; Xiong, X.; Hu, Y. *Environ. Sci. Pollut. Res.* **2016,** *23*, 4489–4497.
[66] Logaranjan, K.; Raiza, A.J.; Gopinath, S.C.; Chen, Y.; Pandia, K. *Nanoscale Res. Lett.* **2016,** *11*, 520.
[67] Kim, J.S.; Kuk, E.; Yu, K.N.; Kim, J.H.; Park, S.J.; Lee, H.J.; Kim, S.H.; Park, Y.K.; Park, Y.H.; Hwang, C.Y.; Kim, Y.K. *Nanome. Nanomed Nanotech Biol. Med.* **2007,** *1*, 95–101.
[68] Shankar, S.; Rhim, J.W. *Carbohydr. Polym.* **2015,** *130*, 353–363.
[69] Borase, H.P.; Patil, C.D.; Sauter, I.P.; Rott, M.B.; Patil, S.V. *FEMS Microbiol. Lett.* **2013,** *345*, 127–131.
[70] Barua, S.; Banerjee, P.P.; Sadhu, A.; Sengupta, A.; Chatterjee, S.; Sarkar, S.; Barman, S.; Chattopadhyay, A.; Bhattacharya, S.; Mondal, N.C.; Karak, N. *J. Nanosci. Nanotechnol.* **2017,** *17*, 968–976.
[71] Greulich, C.; Diendorf, J.; Gessmann, J.; Simon, T.; Habijan, T.; Eggeler, G.; Schildhauer, T.A.; Epple, M.; Köller, M. *Acta Biomater.* **2011,** *7*, 3505–3514.
[72] Kanipandian, N.; Kannan, S.; Ramesh, R.; Subramanian, P.; Thirumurugan, R. *Mater. Res. Bull.* **2014,** *49*, 494–502.
[73] Hackenberg, S.; Scherzed, A.; Kessler, M.; Hummel, S.; Technau, A.; Froelich, K.; Ginzkey, C.; Koehler, C.; Hagen, R.; Kleinsasser, N. *Toxicol. Lett.* **2011,** *201*, 27–33.
[74] El Badawy, A.M.; Silva, R.G.; Morris, B.; Scheckel, K.G.; Suidan, M.T.; Tolaymat, T.M. *Environ. Sci. Technol.* **2011,** *45*, 283–287.